Available online at www.sciencedirect.com
ScienceDirect
Cement and Concrete Research 37 (2007) 386–397
Cement and Concrete Research

New methods to measure liquid permeability in porous materials

George W. Scherer *, John J. Valenza II, Gregory Simmons

Princeton University, Civil and Env. Eng./PRISM, Eng. Quad. E-319, Princeton, NJ 08544, USA

Received 17 March 2006; accepted 24 September 2006

Abstract

Several novel methods have recently been proposed for rapid measurement of the liquid permeability of saturated cement paste, mortar and concrete. The relative merits of the techniques are discussed, and some recent results obtained on pastes and mortars are presented. The low permeabilities seen in cement paste are inconsistent with the pore size distributions measured following drying, indicating that the pore structure is significantly changed by drying.

Keywords: Permeability; Pore size; Tortuosity; Difussion

1. Introduction

The permeability of concrete is related to its durability upon exposure to freeze/thaw cycles [1,2] and crystallization of salts [3]; nevertheless, this property is not routinely measured, because the experiment is difficult. The conventional method for measuring permeability is to establish a pressure gradient over a slab of material and measure the flow through it, but this can take days or weeks for good quality concrete [4], and the sample can be changed (owing to hydration and/or leaching) during that time [5]; moreover, there is a high risk of leaks under pressure that can be hard to detect. Recently, novel techniques have been introduced that permit measurement of low permeabilities in a matter of minutes or hours, so that the evolution of the properties can be followed from early ages. We will review these methods and discuss some typical results; we consider only the liquid permeability of fully saturated materials. Then we will review a variety of theoretical models for permeability and compare them to the data for cement and concrete. The results indicate that the pores controlling flow in cementitious materials are extremely small (<10 nm), so the pore liquid is likely to exhibit anomalous properties.

2. Measuring permeability

The flow of liquid in porous materials obeys Darcy's law [6], which says that the flux is proportional to the gradient in pressure, p:

$$J = -\frac{k}{\eta}\nabla p \tag{1}$$

where k is the permeability (with units of area) and η is the dynamic viscosity of the pore liquid. A commonly used unit for permeability is the *darcy*, which is 10^{-12} m^2; permeabilities of rocks are commonly in the millidarcy to darcy range; cement and concrete fall in the micro- to nanodarcy range. Eq. (1) is often written with the pressure replaced by the hydraulic head, h:

$$J = -k_w \nabla h = -\left(\frac{k\rho_w g}{\eta_w}\right)\nabla h \tag{2}$$

so the permeability k_w is related to k by a product of the properties of water (ρ_w=density and η_w=viscosity) and the gravitational constant, g; at room temperature, the conversion factor is k_w (m/s)= 10^7 k (m^2).

The most obvious way to measure k is to establish a pressure gradient through a sample and measure J using a device such as that in Fig. 1. In one version, a series of concentric o-rings is placed on the upper surface, to permit separate measurement of the flux from several annuli in order to identify heterogeneity in

* Corresponding author.
E-mail address: scherer@princeton.edu (G.W. Scherer).
URL: http://cee.princeton.edu/scherergroup.

0008-8846/$ - see front matter © 2006 Elsevier Ltd. All rights reserved.
doi:10.1016/j.cemconres.2006.09.020

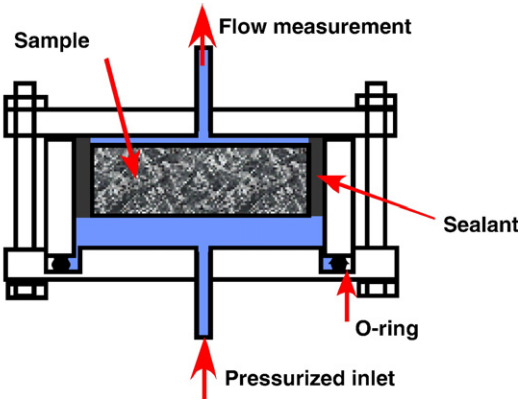

Fig. 1. Schematic design of conventional permeameter. Water or other fluid is injected under pressure (from the bottom, in this case), and the flux is measured from the opposite surface. The sample is sealed into the vessel with a resin, or by a pressurized sleeve (as in a triaxial test).

the sample [7]. The sample must be sealed so that liquid cannot leak around the sides. This may be done by gluing the sample into place with a resin, but this requires drying the surface, which may alter the permeability. Alternatively, a triaxial tester may be used, in which a rubber sleeve is pressurized against the sample; this confinement pressure is recommended to be ~4 times the pressure driving the flow [8]. Since the permeability of cement paste is typically $<10^{-18}$ m^2, such experiments are slow; for example, it takes days to stabilize the flux through a sample with $k_w=10^{-14}$ m/s [4,8]. To accelerate the flow, pressures on the order of MPa may be used, but this increases the risk of leaks that cause an overestimate of k.

In an excellent review, Hooton [9] identifies several factors that must be considered when using this method. First, one must decide whether the relevant permeability is that of a virgin (undried) sample, or one that has previously been dried. This is crucial, because a single drying cycle can raise the permeability of concrete by two orders of magnitude [5]; however, the microcracks responsible for this change will begin to heal during the measurement [10], so the duration of rewetting influences the measured permeability. The mechanical loading history is also important, as stresses exceeding about a third of the compressive strength cause microcracks that raise the permeability [11]. Second, it is essential for the sample to be saturated, which may be difficult or impossible to achieve for low water/cement (w/c) ratios; moreover, the water should be de-aired to prevent pore blocking by bubbles. Third, the confinement pressure must be sufficiently high to prevent leaks; indeed, order-of-magnitude changes can be seen as that pressure is varied. Fourth, concrete samples must be at least three times thicker than the diameter of the largest aggregate, or the flow is dominated by "short-circuits" through the interfacial transition zone [12]. Fifth, exposure of the outlet face results in capillary pressure that can substantially distort the pressure gradient when low pressures are applied. Even when all these factors are properly controlled, the variation in permeability measurements on nominally identical samples is on the order of ±50%.

Pressure relaxation methods involve raising the pressure on one side of a sample and observing the rate of decay of the pressure as liquid drains through the sample [13,14]; while this is much faster, it still requires high pressure apparatus and can be hampered by leaks, or failure to pre-saturate the sample. Eldieb and Hooton compared the permeability obtained using a triaxial cell [4,15] with that obtained by pressure relaxation [16]. They found that they could measure an extremely low permeability ($k_w=10^{-16}$ m/s) in ~30 h with the pressure pulse method, whereas it took ~330 h with the triaxial cell. The duration of the measurement is important for minimizing leaching [5] or hydration [17]; shorter measurements are also desirable for probing the effect of aging on permeability.

An alternative method that was originally developed for gels [18] and later extended to more rigid materials [19,20] is beam bending. When a saturated beam is bent, the top half is compressed and the bottom half is stretched, so a pressure gradient is created in the pore liquid: liquid flows from the top to the bottom within the beam; it also flows out of the top into the surrounding bath, and into the bottom from the bath. As the pore pressure equilibrates, the force required to sustain a fixed deflection decreases, and the kinetics of relaxation of the force can be analyzed to obtain the permeability; additionally, one

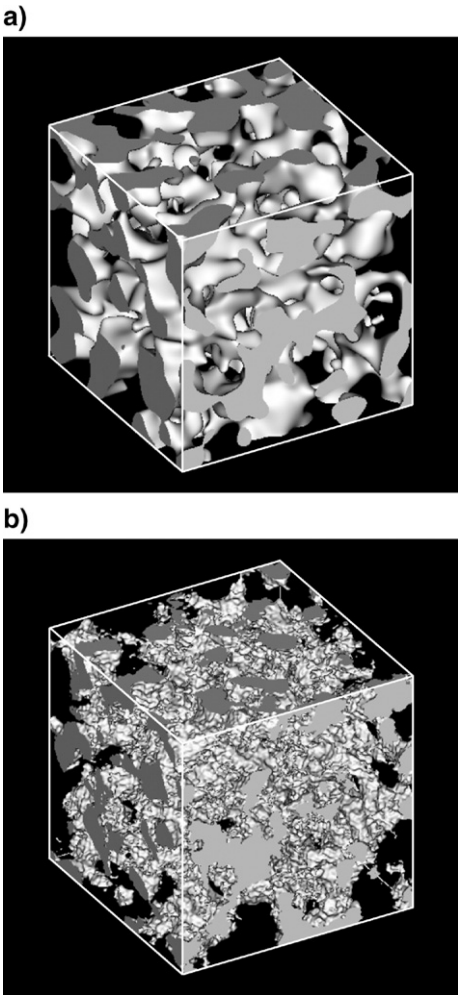

Fig. 2. 3D off-lattice reconstruction of a Vycor-like porous glass. The pore network is in white. The edge of the cube is 100 nm. a) "smooth" interface; b) "rough" interface that reproduces measured surface area. From Ref. [30].

obtains the elastic modulus and the viscoelastic stress relaxation function of the solid phase. The kinetics can be analyzed in closed form using the principles of poromechanics [21], originally developed by Biot [22]. The bending method has been applied to porous glass [23], cement paste [24–26], and mortar [27]. Validation of the method was achieved by comparing the results obtained on Vycor® porous glass [23] with data from the literature [28,29]. A reconstruction of the pore structure of this material is shown Fig. 2 from Levitz [30]. It is made by inducing phase separation in an alkali borosilicate glass, then dissolving the alkali borate phase in acid, leaving almost pure silica [31]. Typically, the pore diameter is ~5 nm with a very narrow distribution, porosity is ~30%, and surface area is 130–200 m^2/g, but there are significant batch-to-batch variations. Bending experiments were performed on samples saturated with a range or *n*-alcohols and water to test the theoretical prediction of the influence of the viscosity and compressibility of the pore liquid. The force, *W*, required to sustain a fixed deflection on the beam is predicted to relax according to

$$\frac{W(t)}{W(0)} = 1 - A + AS(t/\tau_b) \tag{3}$$

where A is a constant given by

$$A = \frac{1-2\nu_p}{3[1 + K_p/(Mb^2)]} \tag{4}$$

and M is the Biot modulus, defined as [21]

$$\frac{1}{M} = \frac{\phi}{K_L} + \frac{b-\phi}{K_S} \tag{5}$$

in which ν_p=Poisson's ratio of the drained porous body, φ=porosity, K_L=bulk modulus of the pore liquid, K_p=bulk modulus of the drained porous body, K_S=bulk modulus of the solid phase(s) constituting the body, and b is the Biot coefficient, defined as $b = 1 - K_p/K_S$. For a soft material, such as a gel, $K_p \ll K_S$, so $b \approx 1$ and $K_p/M \approx 0$; however, for porous glass or cementitious materials, b is on the order of 0.4–0.7. The relaxation function in Eq. (3) depends on the shape of the beam [19,20]; for a square beam, it conforms exactly to the data shown in Fig. 3b. The hydrodynamic relaxation time, τ_b, governs the rate of equilibration of the pore pressure. For a cementitious material, in which K_p and $K_S \gg K_L$, it is given approximately by[1]

$$\tau_b \approx \left(\frac{\eta a^2}{k}\right)\left(\frac{\phi}{K_L}\right) \tag{6}$$

where a is the half-thickness of the beam. Eq. (6) indicates that the rate of relaxation depends on the viscosity and compressibility of the pore liquid, and this is reflected in the shift of the curves in Fig. 3. When they are shifted vertically according to Eq. (4) and horizontally according to Eq. (6), all the data converge onto a single curve, whose shape is $S(t/\tau_b)$. The permeability calculated from Eq. (6) is in good agreement with values obtained by the conventional method on a similar sample by Debye and Cleland [28], confirming that the bending method correctly yields the permeability. The bending data also agree with the earlier work in that the permeability varies systematically with the molecular size of the pore liquid. By assuming that a monolayer of solvent is immobilized on the pore wall for the organic liquids, and two layers (0.5 nm) for water, the variation in permeability can be explained, as shown in Fig. 4. We will return to the question of mobility of water near solid surfaces in the Discussion.

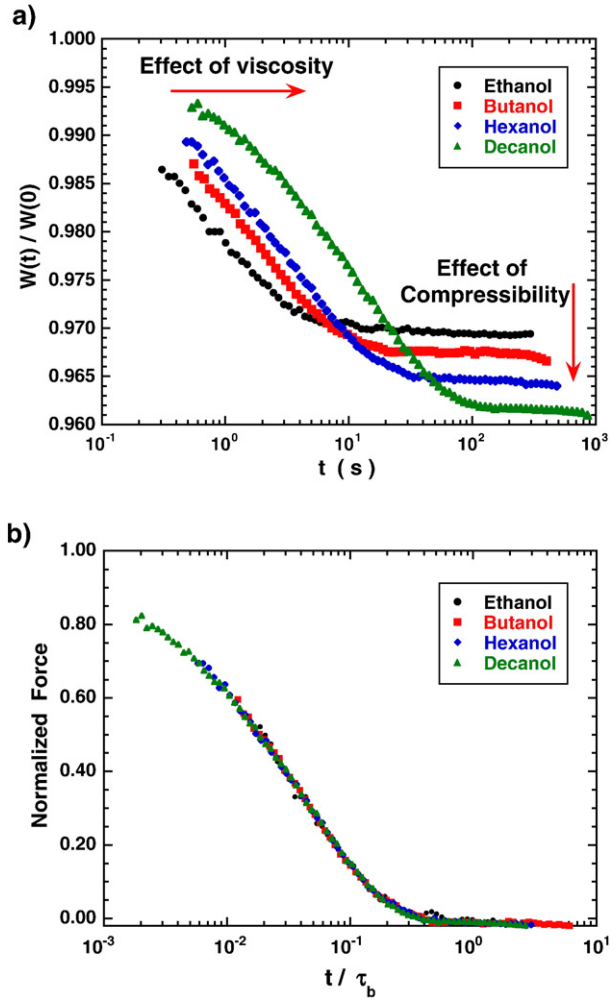

Fig. 3. Normalized force, $W(t)$, required to hold fixed deflection on a square beam of Vycor® porous glass saturated with the indicated liquids. a) The rate of relaxation decreases as the viscosity increases, and the amount of relaxation increases with the compressibility. b) When these factors are taken into account according to the analytical theory [19], all of the curves collapse onto the predicted shape; τ_b is the hydrodynamic relaxation time for equilibration of the pore pressure. Data from Ref. [23].

[1] It has been shown that the hydrodynamic relaxation time must have a certain form (see Eqs. (5.21–5.22) of Ref. [21]) that differs from the result given in Ref. [19], which must be inexact. The most likely reason for this discrepancy is the approximate nature of the strains in the beam that are deduced from simple beam theory (O. Coussy, private communication). The equations from Refs. [19,21] both lead to the result given in Eq. (6), so the quantitative error is negligible for cementitious materials. Even for gels, where the difference is expected to be significant, the permeability extracted from bending experiments agrees well with independent measurements. Therefore, it is likely that the use of simple beam theory introduces offsetting errors in the relaxation time and the relaxation function, such that the measured permeability is correct. This is confirmed through finite element analysis [G.W. Scherer and J. H. Prévost, work in progress].

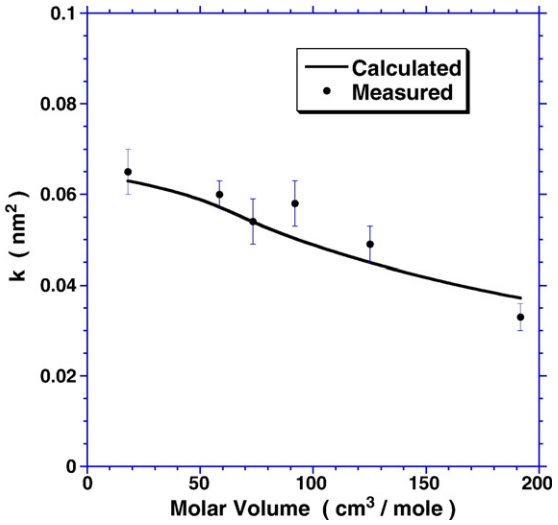

Fig. 4. Symbols are measured permeability values for various liquids in Vycor®, taken from erratum listed in Ref. [23]. Curve is calculated using the Carman–Kozeny equation, as explained in Ref. [23], except that the thickness of immobilized water is taken to be 0.5 nm, rather than a single molecular diameter.

Bending has also been applied to measure the permeability of cement paste [24–26] with a range of *w*/*c* and curing times. In fact, hydrodynamic relaxation in bending of cement paste had been seen and understood by Sellevold and Richards [32], although they did not exploit it to measure permeability. In contrast to Vycor®, cement paste is viscoelastic, so the measurement also yields the stress relaxation function. A two-parameter relaxation function was originally developed for paste samples from 1 to 4 days old [25], but it has subsequently been found to describe paste at least one year old, as well as mortar [27]. An example of a relaxation curve for mortar is shown in Fig. 5, together with the hydrodynamic relaxation curve (*i.e.*, the equilibration kinetics of the pore pressure) and the viscoelastic relaxation extracted from the data. The permeability is determined from a fit of the data to the theoretical function; the hydrodynamic and viscoelastic effects are easily separated, as long as the inflection in the curve, which reflects the end of the hydrodynamic relaxation, is visible. For this mortar, the inflection occurs after about 4 min, so the results are obtained very quickly even though k is only $\sim 3\times10^{-21}$ m^2. The experiment was continued for 3 h, so that the shape of the relaxation function could be established. The permeability of the mortar was larger than that of the corresponding paste, in spite of the high loading of impermeable sand, so the interfacial transition zone was obviously important to the transport process.

Several important precautions must be taken in this method. First, the sample must be long and slender (length/thickness at least 10, but preferably ≥ 20), so that simple bending theory is valid and indentation by the supports is minimal. Second, the beam must be thick enough so that it represents the bulk properties of the material of interest. Only a few millimeters are needed for porous glass, paste, mortar, stone, and other relatively homogeneous materials, but not for concrete. Third, the sample must be fully saturated, so that the pore pressure is relieved by flow to the exterior surface, rather than by compressing pockets of air. An excellent test of saturation is obtained by using samples of several thicknesses to confirm that the hydrodynamic relaxation time varies as thickness squared, as predicted by Eq. (6). By that method, it was demonstrated that paste cylinders thicker than ~8 mm contain enough trapped air to interfere with the measurement. However, by submerging the rods in water and subjecting them to ~2 MPa pressure, the air was dissolved and the dependence of τ_b on a^2 was demonstrated for cylinders up to 12 mm in diameter. During the measurement, the sample remains immersed in a bath containing the same liquid that is in the pores of the specimen, so no drying or leaching occurs. Fourth, the strain must be small enough to avoid damage. In the study of cement paste [24] the strain was $<10^{-4}$, and repeated measurements demonstrated that there was no change in permeability attributable to microcracks.

Clearly the beam-bending method is extremely rapid, and it provides the viscoelastic properties, as well as the permeability, so it is an ideal method for characterizing a material that can be prepared in the form of a slender beam. In particular, it is useful for studying the evolution of the properties at young ages, since the duration of the experiment is short [25]. In principle, it could also be used for concrete, but the samples would have to be inconveniently large (say, 10 cm thick and more than a meter long). Fortunately, other fast methods exist that do not have the same geometrical limitations.

Thermopermeametry (TPA) is another method that was first applied to gels [33,34] and later extended to more rigid materials, such as cement paste [35,36]. The original elastic analysis was found to be inadequate for cement paste, so a viscoelastic analysis was developed [37] and shown to describe the thermal expansion kinetics of saturated paste [38,39]. The principle of the method is that the thermal expansion of the pore liquid is always much greater than that of the solid phase, so when the body is heated the expanding liquid no longer "fits" in the pores;

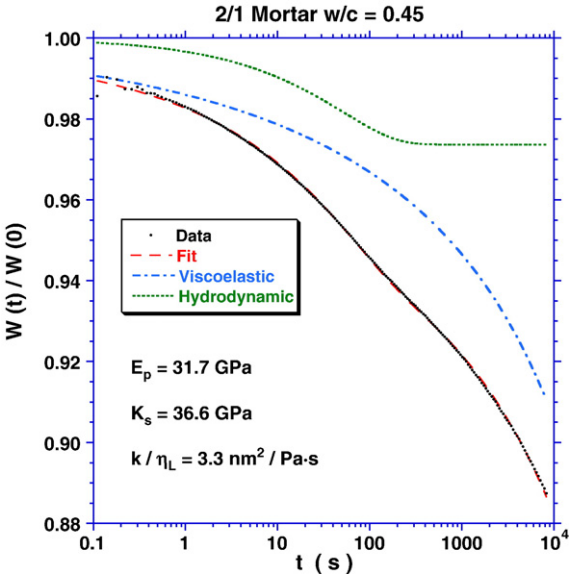

Fig. 5. Relaxation of force, W, on mortar beam (2 parts sand/1 part cement, water/cement ratio = 0.45) as a function of time, t, after deflection was imposed. Symbols (●) are data, and dashed curve is fit to data, which is the product of the hydrodynamic relaxation (dotted curve) and the viscoelastic relaxation of the solid phase (dash–dot curve).

if it does not have time to flow out of the body as the temperature rises, it expands within the pores and stretches the solid phase. The solid gradually squeezes the liquid out of the pores at a rate controlled by the permeability, so by measuring the kinetics of expansion of the body, one can determine the permeability. An example of a thermal expansion curve for cement paste is shown in Fig. 6. (This measurement was made using a special dilatometer [38], but comparable results can be obtained on small samples of homogeneous materials in a dynamic mechanical analyzer [39], as long as the sample is immersed.) If the same thermal cycle had been applied to the dry solid body, the strain would have followed the dashed curve labeled $\alpha_S\ \Delta T$, but the pore liquid causes an overshoot and undershoot following heating and cooling, respectively. The overshoot had been seen previously [40–42] and explained in terms of expansion of the liquid [43]. Here we see that there is also an undershoot, indicating a negative pressure in the pore liquid, which is possible only if the sample is fully saturated (otherwise, the suction is relieved by bubble growth, rather than contraction).

In principle, this technique can be applied to large samples, such as the cylinders routinely used for strength measurements of concrete. It has the advantage of being much faster than conventional methods, and does not require the slender samples needed for beam bending. Unfortunately, while this method works well for gels and cement paste, recent experiments with mortars [27] revealed that entrapped air seriously compromised the results, because the pore pressure can be relieved by flow into the air pockets. Since the spatial distribution of the air voids is unknown, the kinetics of relaxation cannot be interpreted quantitatively. Efforts were made to pre-saturate the samples by submerging them in limewater and exerting 2–3 MPa of pressure to collapse and dissolve the air bubbles. This was effective, but it took as much as 3 weeks to saturate mortar cylinders that were only 4 cm in diameter. If the samples were prepared under vacuum (to eliminate gas pockets) or under a

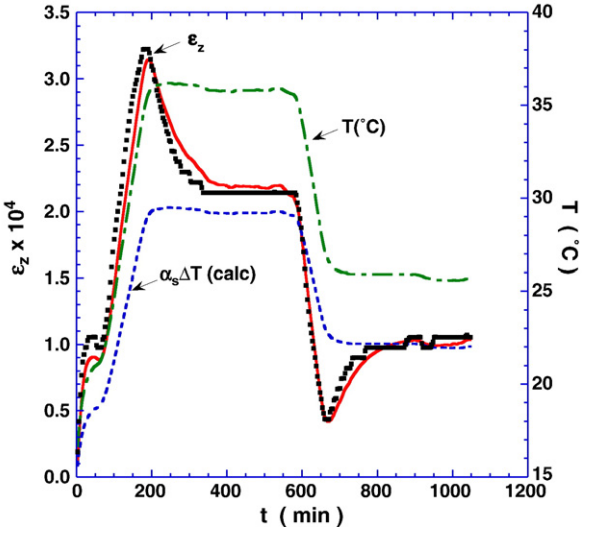

Fig. 6. Axial strain (left ordinate) of cylinder (19 mm diameter) of cement paste (Type III, $w/c=0.5$) subjected to thermal cycle (right ordinate). Black symbols are the measured strain and the continuous curve is the best fit to the theory from Ref. [37]. From Ref. [38].

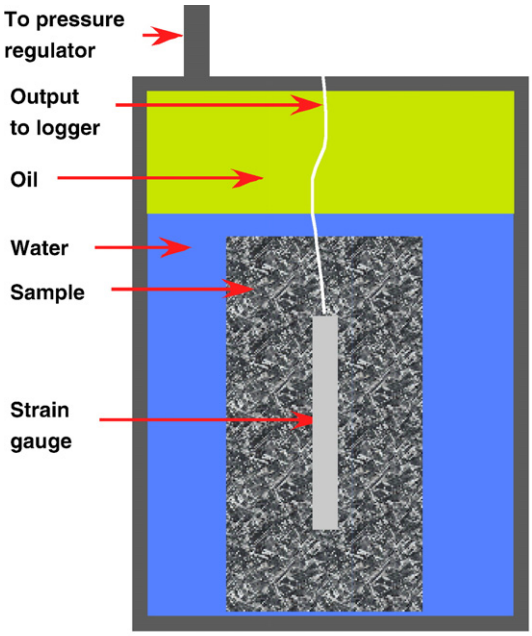

Fig. 7. Schematic of system used for dynamic pressurization measurement. Sample containing embedded strain gauge is immersed in lime-saturated water, then covered with oil. Pressure is suddenly applied to the oil and the strain of the sample is continuously monitored.

flow of CO_2 (to ensure that only highly soluble gas is present), then saturation could be achieved more rapidly and TPA could be used. This approach has been successful with larger samples tested with the dynamic pressurization method described next; however, it does not appear that either method could be applied to routine strength cylinders, which always contain some entrained and/or entrapped air.

Another method for measuring permeability is dynamic pressurization, which was first applied to aerogels [44] and has recently been extended to cement paste [45–47]. (A similar method has also been applied for measuring permeability to gas [48].) In this case, a saturated sample is submerged in a bath within a pressure vessel (see Fig. 7), then the bath is suddenly pressurized: the sample immediately contracts by an amount that depends on the undrained bulk modulus, K_u:

$$\varepsilon_0 = -\frac{p_A}{3K_u} \tag{7}$$

where

$$K_u = K_p + b^2 M = K_p + b^2 / \left(\frac{\phi}{K_L} + \frac{b-\phi}{K_S} \right). \tag{8}$$

As the liquid from the bath penetrates the pores, the rising pore pressure causes the body to re-expand. The final dimensions of the body depend on the bulk modulus of the solid phase (not the drained modulus of the porous body), and the kinetics of re-expansion reveal the permeability. A simple closed-form expression describes the kinetics following a step change in applied pressure, p_A:

$$\varepsilon_z = \varepsilon_\infty + (\varepsilon_0 - \varepsilon_\infty)\Omega(t/\tau_v) \tag{9}$$

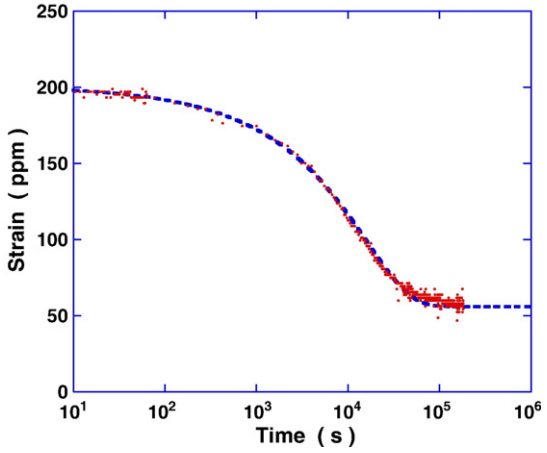

Fig. 8. Strain data (symbols) and fit to theoretical expression (dashed curve) in a dynamic pressurization experiment on a Type III cement paste ($w/c=0.5$) subjected to 6.9 MPa of hydrostatic pressure. From Ref. [46].

where Ω is the relaxation function; the final strain is

$$\varepsilon_\infty = -\frac{p_A}{3K_S} \tag{10}$$

The permeability can be found by fitting the measured strain to Eq. (9) using the known form [45] of the relaxation function, as shown in Fig. 8. This method has been found to work well on cement paste and concrete, as indicated by the data in Fig. 9. The permeability values from dynamic pressurization [46] compare very well with data from beam bending made on the same type of cement [24]. Samples 9 cm in diameter with permeabilities $\sim 3\times10^{-14}$ m/s can be measured in the course of a day. As in the case of TPA, this method requires the body to be free of air voids. Fig. 10 shows the calculated axial strain of a cylinder as a function of the volume percentage of entrapped air, indicating that the time required for re-expansion is ~5 times as long when the pores contain 3% air. In contrast to TPA, the experiment directly indicates the presence of air, because the strains measured during pressurization and depressurization should be symmetrical; if they are not, then air pockets must be present. The cycles can be repeated until the air dissolves and the data are reproducible. A more effective approach is to mix the sample under vacuum to avoid entrapping air, as was done in preparing the samples used to generate the data in Figs. 8 and 9. Another important consideration is that the pressure jump should not do damage to the sample. This is not a serious limitation during a compressive step, but it is easy to do damage during depressurization, because this creates tensile stress in the sample equal to $\sim p_A/2$ [45]. Therefore, one should make measurements only during compression, and depressurize slowly, or use pressure jumps significantly smaller than the tensile strength of the sample. For best accuracy, the ends of the sample should be sealed, because the theory assumes that the flow into the sample is purely radial.

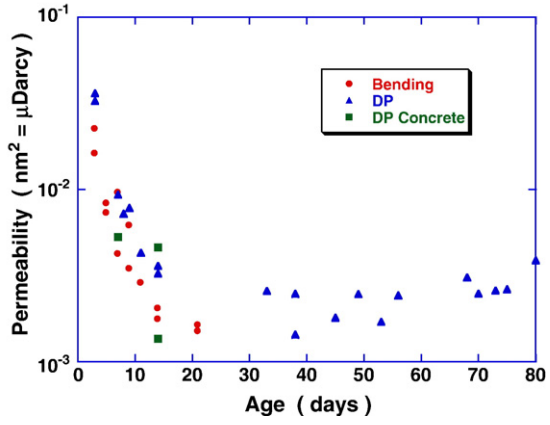

Fig. 9. Permeability values for Type III cement paste ($w/c=0.5$) obtained using beam-bending (Bending) or dynamic pressurization (DP); square symbols are from DP measurements on concrete made from the same cement with 482 kg/m^3 (809 lb/yd^3) of paste. Data from Refs. [24] (Bending) and [46] (DP).

3. Models of permeability

The simplest possible model for flow in porous media is a bundle of parallel non-intersecting cylinders with radius r, each carrying a flow Q (volume/time) given by Poiseuille's law [6]:

$$Q = -\frac{\pi d^4}{128\eta}\nabla p \tag{11}$$

If there are n such pipes per unit area, the flux is

$$J = nQ = -\frac{n\pi d^4}{128\eta}\nabla p = -\frac{\phi d^2}{32\eta}\nabla p \tag{12}$$

where $\varphi = n\pi\, d^2/4$ is the porosity. Comparison of Eq. (12) with Eq. (1) indicates that the permeability of a body consisting of straight pipes is

$$k_{SP} = \frac{\phi d^2}{32} \tag{13}$$

Thus, we expect the permeability to be related to the porosity and the cross-sectional area of a pore. Of course, the pores in real materials are non-circular, intersecting, and tortuous, so Eq. (13) must be modified to take account of those details. The

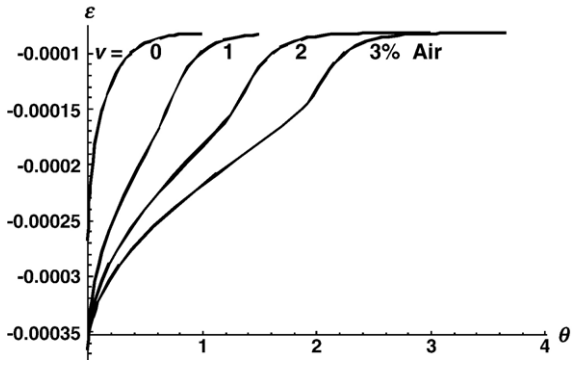

Fig. 10. Calculated axial strain in a cylinder of cement paste when the pores contain water contaminated with various volume percentages, v, of air. The abscissa is a dimensionless time scale, normalized by a quantity related to the permeability and modulus of the material.

simplest approach is to insert a "finagle factor" called the Kozeny constant, κ, (which is actually somewhat density dependent [49]) into the denominator:

$$k_k = \frac{\phi d^2}{16\kappa} \tag{14}$$

For a wide range of porous materials, Eq. (14) is found to work quite well with $\kappa \approx 5$ [6]. This formula has been successfully tested against simulations of flow through various obstacles [6], and it appears to work particularly well when the obstacles are disordered or fractal [50]. The Kozeny formula was found to work very well for gels, where the permeability was measured by beam bending and the pore diameter was obtained by nitrogen desorption [51,52]. If Eq. (14) is used with the measured porosity (0.315) and the pore size found by nitrogen desorption (d=5.4 nm) for Vycor® glass, the result is k_K=0.11 nm^2, which is about twice as large as the measured values; if the hydraulic diameter is used (d_h=4 V_p/S=3.3 nm, based on a surface area of 131 m^2/g and pore volume of 0.216 cm^3/g), the calculated value rises to k_K=0.17 nm^2. The good results in Fig. 4 were obtained by reducing the pore diameter by the thickness, δ, of a molecular layer of pore liquid presumed to be immobile against the pore wall; the porosity was also reduced by $\delta S \rho_b$, where S is the measured surface area and ρ_b is the bulk density. The existence of one or two layers of surface-affected pore liquid is supported by spectroscopic data [53], neutron scattering [54], and numerous molecular dynamics simulations [*e.g.*, [55,56]], as well as studies of transport properties [28].

Katz and Thompson (K–T) [57,58] introduced a formula for permeability based on percolation theory:

$$k_{KT} = \frac{d_c^2}{226F} = \frac{\phi d_c^2}{226\tau} \tag{15}$$

where $F=\varphi/\tau$ is called the formation factor and τ is the tortuosity; the characteristic pore diameter, d_c, is the breakthrough diameter, which can be estimated from the peak of the pore size distribution found by mercury intrusion. Johnson et al. [59] introduced a more rigorous choice for d_c, obtained by weighting the surface/volume ratio by the intensity of the electric field in the pores; however, the derivation is only expected to be valid when the pores are large enough so that surface-affected layers are small compared to the pore size. In fact, Eq. (15) was developed and verified for stone, which has micron-sized pores, so modifications are likely to be necessary for nanometric pores.

The tortuosity can be obtained by measuring the diffusion coefficient in the pore liquid, D, and comparing it to the self-diffusion coefficient in the bulk liquid, D_0 [60]:

$$\frac{D}{D_0} = \frac{1}{\phi F} = \frac{1}{\tau} \tag{16}$$

Using NMR, the diffusion coefficient of water was measured in the same sample of Vycor® that was used for the beam-bending experiments [61], with the result τ=4.8, which is consistent with values reported in the literature for similar glasses [29,30]. Using this value with the hydraulic diameter, Eq. (15) yields k_{KT}=0.012 nm^2, which is ~20% of the value for water (~0.065 nm^2) in Fig. 4. Reducing the pore diameter by 1 nm to account for the immobile water layer decreases k_{KT} to 0.008 nm^2. Evidently, this equation does not work well for Vycor®. We will now consider how well the Kozeny and K–T equations work for cement and concrete.

4. Discussion

A surprising observation made during TPA measurements on cement paste is that the thermal expansion coefficient of the pore liquid is 30–50% larger than that of bulk water at ambient temperature [39]. Direct dilatometric measurements show that similarly elevated expansion coefficients are found in porous glass, when the pore diameter is below ~15 nm [62,63]. Recent molecular dynamics simulations of water in a narrow slit [64] yield expansion values in excellent agreement with measurements in silica xerogels [65]. Therefore, the expansion coefficient in cement paste implies that the water is in pores with diameters below ~10 nm. However, pore size distributions measured on cement paste using mercury intrusion or nitrogen desorption generally indicate that the pores lie between 10 and 100 nm (or larger) [66–68], so the expansion behavior seems to be dominated by a small fraction of the pores with small diameters. Even more surprising is the inconsistency between the low permeability of cement paste and the reported pore size range. Given $k=10^{-21}$ m^2 and φ=0.3, Eq. (14) predicts a pore diameter of ~0.5 nm. Obviously, this is orders of magnitude smaller than the pore sizes measured by the usual methods. Since the structure of the liquid is sufficiently altered to raise the thermal expansion coefficient, one might argue that the viscosity is anomalously high in the pores of the paste, so that k is underestimated if the bulk viscosity is used in the calculation. The measurements on porous glass described earlier suggest that there is a monolayer of immobilized liquid molecules on the surface of the solid phase, so the effective pore size is correspondingly reduced; however, the rest of the liquid in the pores appears to have normal viscosity. This is supported by molecular dynamics simulations that indicate a normal structure for water molecules lying more than 0.5 nm from a silica surface [64]. It seems likely that the pore structure of cement paste obtained from mercury intrusion or nitrogen desorption is an artifact of the drying that precedes the measurement.

Several attempts have been made to apply the Katz–Thompson equation to cement paste. Garboczi [69] concluded that the model worked, but he had to assume a tortuosity of 570, which is an order of magnitude greater than the values found from electrical measurements on comparable materials [70]. Baroghel-Bouny et al. [71] reported order-of-magnitude agreement with the K–T equation for pastes with permeabilities on the order of 10^{-14} m/s, which were inferred from the drying kinetics. The formation factor from diffusivity of Cl^- in paste was $F \approx 1800$ for a high-performance paste (w/c=0.19 with 10% silica fume) and $F \approx 300$ for ordinary paste (w/c=0.34); the pore diameters from mercury penetration were respectively 8.6 and 20 nm [72]. El-Dieb and Hooton [73] performed an extensive test of the K–T equation, using permeability data on

paste and concrete, along with mercury intrusion data. As shown in Fig. 11, the correlation was quite poor for paste, with the calculated permeabilities orders of magnitude greater than the measured values. The results for concrete were even worse. Tumidajski and Lin [74] made a similar comparison, but found the K–T values to be ~100 times *lower* than the measured permeabilities; however, they had improbably high permeabilities (10^{-8}–10^{-10} m/s), so there may have been an error in their data for k_w.

If we use the Kozeny equation to estimate the pore size of cement paste, then it is reasonable to replace d with $d-\delta$ and reduce the porosity by $\delta S \rho_b$, as was done for the Vycor® data:

$$d \approx \delta + \sqrt{\frac{80k}{\phi - \delta S \rho_b}} \tag{17}$$

Using $\delta = 0.5$ nm and $S = 100$ m^2/g, with the measured densities, and permeability data obtained on paste by beam bending [24], we obtain the pore diameters shown in Fig. 12, which range from about 1.5 to 5 nm; changing the choice of S within the observed range (~60–200 m^2 [75]) would not shift the values substantially. The implication is that the permeability is controlled by the "gel pores", rather than the capillary pores in the paste. How can we reconcile this result with the pore sizes measured by mercury porosimetry?

The basic problem with mercury porosimetry and nitrogen sorption is that the samples must be severely dried before measurement. Since the permeability is known to leap by two orders of magnitude after drying [5,9], the effective pore diameter must increase substantially. Therefore, it is inappropriate to interpret the permeability of virgin samples on the basis of pore sizes determined on dried samples. Moreover, the high pressure exerted during mercury intrusion can damage the sample, particularly when entering the smaller pores [76]. An additional problem, in the case of concrete, is the small size of

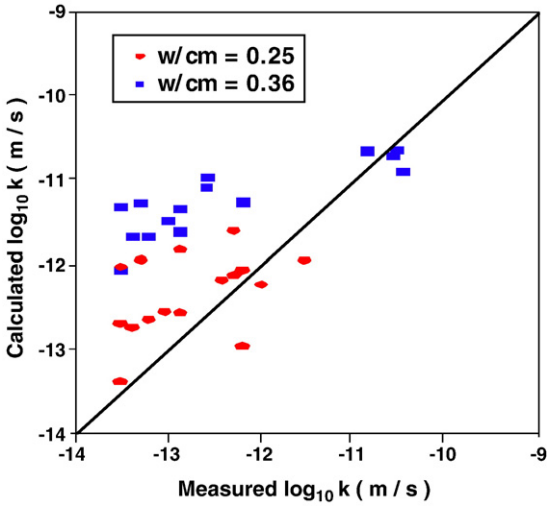

Fig. 11. Comparison of measured permeability of cement paste with values calculated using the Katz–Thompson equation, together with microstructural information from mercury intrusion. Data from Ref. [73].

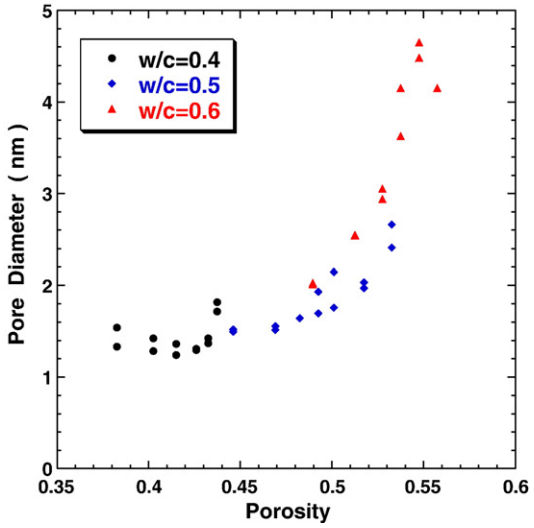

Fig. 12. Pore diameters calculated from Eq. (17), using permeability data for cement paste (Type III, $w/c = 0.4$, 0.5, and 0.6) from Ref. [24].

the sample. It has been reported that the permeability is much greater when the sample thickness is less than ~3 times the aggregate diameter [12], presumably because this raises the likelihood of interfacial transitions zones percolating through the sample. Similarly, intrusion of a small sample will exaggerate the role of the ITZ. These issues help to explain the failure of comparisons of measured permeabilities with values calculated from the K–T equation, where the pore sizes are taken from mercury intrusion.

Fortunately, there are methods for measuring pore sizes that do not require drying, including nuclear magnetic resonance (NMR) relaxation time analysis [77–80] and thermoporometry (TPM) [81–83]. Scattering methods also give useful structural information, but not a pore size distribution [75]. NMR is particularly attractive, because it can provide information on the hydration reaction, image the distribution of moisture and salts during drying, and measure diffusion coefficients in the pore liquid, in addition to providing pore sizes [84]. Although NMR is capable of seeing much larger pores, studies of cement indicate pores smaller than ~10 nm [77,80]. Thermoporometry exploits the depression in melting point caused by the curvature of ice crystals confined in small pores (i.e., the Gibbs–Thompson effect [2]). If a saturated sample is gradually frozen, the temperature at which ice appears indicates the size of the pores, and the heat released is proportional to the volume of ice formed. Freezing is usually detected calorimetrically, but it can also be done elegantly using NMR [78,85,86]. A particularly interesting study was done by Villadsen [83], who performed calorimetric TPM on very mature cement pastes that had not been dried; he then dried and resaturated them and repeated the measurement. Some of his results are reproduced in Fig. 13a–d. Parts (a) and (b) show the pore size distributions measured in a paste with $w/c = 0.4$; the TPM curve in (b) is shifted to the right, compared to (a), because the sample was dried and resaturated. The virgin sample had no pores with diameters larger than ~6 nm, but the pore sizes double after drying. Similar results are seen in (c) and (d) for a paste with $w/c = 0.6$. Even at that

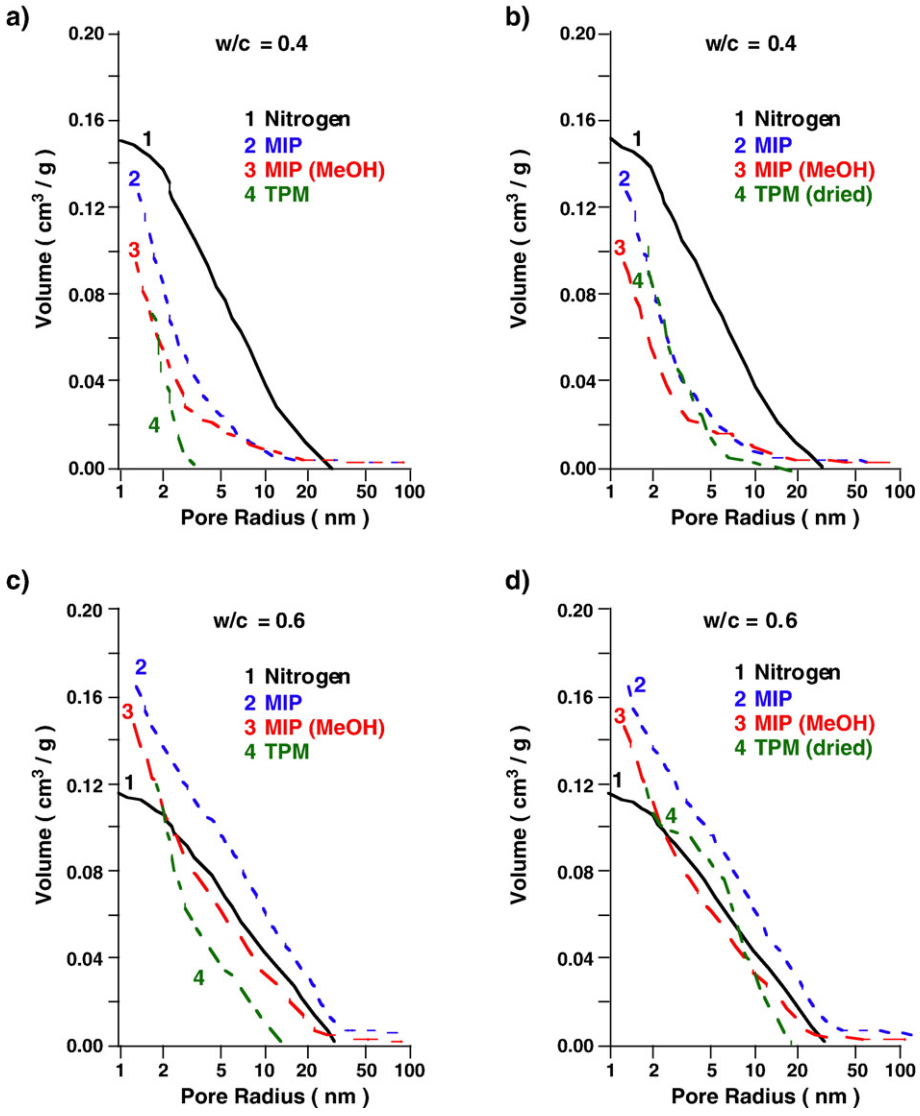

Fig. 13. Pore size distributions in very mature cement paste with $w/c = 0.4$ and 0.6, measured by nitrogen desorption (Nitrogen), mercury intrusion porosimetry (MIP), and thermoporometry (TPM); some of the MIP samples were dried after exchange into methanol (MeOH). In (a) and (c), the TPM samples had not been dried, but in (b) and (d), they were dried and resaturated; this resulted in a shift of the TPM curves toward the others.

high water content, the virgin sample has no pores larger than 30 nm before drying; the shift after drying is not as great in this case, presumably because the larger pores in this paste result in lower capillary pressure [87].

5. Conclusions

Several novel permeability measurements have been introduced that permit relatively rapid measurement, so that the properties of the sample do not change substantially during the test. For homogeneous materials, such as paste and mortar, the beam-bending test is ideal, because it is fast (minutes to hours) and it also provides the elastic and viscoelastic properties of the paste. For concrete, the pressure decay method introduced by Brace et al. [13] is the most attractive of the conventional approaches, because it is relatively fast. However, it still requires high pressures, and therefore presents the risk of leaks, and it gives errors if the sample is not fully saturated. Thermopermeametry is faster and does not require high pressure apparatus; however, the sample must be fully saturated (which can be problematic for high-performance concrete), and some error is introduced by our lack of knowledge about the thermal expansion coefficient of the pore liquid in cement paste. Nevertheless, if saturation can be achieved, this is a relatively easy and quick method. Another rapid method is dynamic pressurization. Although it employs a high pressure chamber, there is no problem with leaks; it is only necessary to hold the pressure constant (even if that requires a continuing addition of fluid to the chamber). As with the other methods, the major difficulty is ensuring full saturation; an advantage of dynamic pressurization is that the shape of the curve indicates whether or not entrapped air is present.

When the measured permeability of cement and concrete is compared to various theoretical models, the agreement is often poor. This is attributed to the inappropriate use of pore size information from dried samples, whose structure is quite

different from that of the undried samples used to measure k. If the theories are used to infer the pore size, the resulting diameters are <5 nm. In fact, pores of this size are found from techniques, such as NMR and thermoporometry, that do not require drying of the sample. Therefore, it is essential to use such methods to obtain pore characterization for prediction of k for virgin cement and concrete.

The practical reason for permeability measurements is to predict the durability of exposed concrete on buildings and road surfaces, which is dry to a depth of some centimeters. In such cases, it is preferable to dry the sample before measuring k; this is particularly important for making conservative predictions, since k may rise one hundred fold after drying. Mechanical loads can also cause microcracks that raise k, so appropriately preloading a sample before measuring permeability is also wise. An issue that has not received enough attention is the effect of microcracks on permeability, and the healing of microcracks in moist environments. For the comparison of experiment and theory, measuring k on dried and resaturated samples is desirable, since the characterization of the pore structure is much easier on dried materials. However, the high permeability of dried materials results from microcracks, whose shape and connectivity are probably qualitatively different from that of the original pores in the undried body.

Acknowledgments

This work was supported by a grant from the National Science Foundation, Division of Civil and Mechanical Systems, grant CMS-0070092. The author is indebted to Profs. Pierre Levitz and Sal Torquato for their helpful discussions of the tortuosity.

References

[1] M. Pigeon, R. Pleau, Durability of Concrete in Cold Climates, E & FN Spon, London, 1995.
[2] G.W. Scherer, J.J. Valenza II, Mechanisms of Frost Damage, in: J. Skalny, F. Young (Eds.), Materials Science of Concrete, vol. VII, American Ceramic Society, 2005, pp. 209–246.
[3] G.W. Scherer, Stress from crystallization of salt, Cem. Concr. Res. 34 (2004) 1613–1624.
[4] A.S. El-Dieb, R.D. Hooton, Water-permeability measurement of high performance concrete using a high-pressure triaxial cell, Cem. Concr. Res. 25 (6) (1995) 1199–1208.
[5] T.C. Powers, L.E. Copeland, M. Mann, Capillary Continuity or Discontinuity in Cement Pastes, J. Portland Cem. Assoc. Res. Dev. Lab. (May 1959) 38–48.
[6] J. Happel, H. Brenner, Low Reynolds Number Hydrodynamics, Martinus Nijhoff, Dordrecht, 1986.
[7] S.A. Jefferis, R.J. Mangabhai, The divided flow permeameter, in: L.R. Roberts, J.P. Skalny (Eds.), Pore Structure and Permeability of Cementitious Materials, vol. 137, Materials Research Society, Pittsburgh, PA, 1989, pp. 209–214.
[8] A.S. El-Dieb, R.D. Hooton, A high pressure triaxial cell with improved measurement sensitivity for saturated water permeability of high performance concrete, Cem. Concr. Res. 24 (5) (1994) 854–862.
[9] R.D. Hooton, What is needed in a permeability test for evaluation of concrete quality? in: L.R. Roberts, J.P. Skalny (Eds.), Pore Structure and Permeability of Cementitious Materials, vol. 137, Materials Research Society, Pittsburgh, PA, 1989, pp. 141–149.
[10] T.A. Bier, D. Ludirdja, J.F. Young, R.L. Berger, The effect of pore structure and cracking on the permeability of concrete, in: L.R. Roberts, J.P. Skalny (Eds.), Pore Structure and Permeability of Cementitious Materials, vol. 137, Materials Research Society, Pittsburgh, PA, 1989, pp. 235–241.
[11] N. Banthia, A. Biparva, S. Mindess, Permeability of concrete under stress, Cem. Concr. Res. 35 (2005) 1651–1655.
[12] R.D. Hooton, L.D. Wakeley, Influence of test conditions on water permeability of concrete in a triaxial cell, in: L.R. Roberts, J.P. Skalny (Eds.), Pore Structure and Permeability of Cementitious Materials, vol. 137, Materials Research Society, Pittsburgh, PA, 1989, pp. 157–164.
[13] W.F. Brace, J.B. Walsh, W.T. Frangos, Permeability of Granite under High Pressure, J. Geophys. Res. 73 (1968) 2225–2236.
[14] P.A. Hsieh, J.V. Tracy, C.E. Neuzil, J.D. Bredehoeft, S.E. Silliman, A transient laboratory method for determining the hydraulic properties of "tight" rocks I. Theory, J. Rock Mech. Min. Sci. Geomech. Abstr. 18 (1981) 245–252.
[15] A.S. El-Dieb, R.D. Hooton, A high pressure triaxial cell with improved measurement sensitivity for saturated water permeability of high performance concrete, Cem. Concr. Res. 24 (5) (1994) 854–862.
[16] R.D. Hooton, A.S. El-Dieb, Evaluation of water permeability of high performance concrete, in: K. Sakai, N. Banthia, O.E. Gjørv (Eds.), Concrete Under Severe Conditions, vol. 1, EF&N Spoon, London, 1995, pp. 423–432.
[17] B.K. Nyame, J.M. Illston, Relationships between permeability and pore structure of hardened cement paste, Mag. Concr. Res. 33 (116) (1981) 139–146.
[18] G.W. Scherer, Bending of gel beams: method of characterizing mechanical properties and permeability, J. Non-Cryst. Solids 142 (1–2) (1992) 18–35.
[19] G.W. Scherer, Measuring permeability of rigid materials by a beam-bending method: I. Theory, J. Am. Ceram. Soc. 83 (9) (2000) 2231–2239; Erratum, J. Am. Ceram. Soc. 87 (8) (2004) 1612–1613.
[20] G.W. Scherer, Measuring permeability of rigid materials by a beam-bending method: IV. Transversely isotropic plate, J. Am. Ceram. Soc. 87 (8) (2004) 1517–1524.
[21] O. Coussy, Poromechanics, Wiley, West Sussex, England, 2004.
[22] M.A. Biot, General theory of three-dimensional consolidation, J. Appl. Phys. 12 (1941) 155–164.
[23] W. Vichit-Vadakan, G.W. Scherer, Measuring permeability of rigid materials by a beam-bending method: II. Porous Vycor, J. Am. Ceram. Soc. 83 (9) (2000) 2240–2245; Erratum, J. Am. Ceram. Soc. 87 (8) (2004) 1614.
[24] W. Vichit-Vadakan, G.W. Scherer, Measuring permeability of rigid materials by a beam-bending method: III. Cement paste, J. Am. Ceram. Soc. 85 (6) (2002) 1537–1544; Erratum, J. Am. Ceram. Soc. 87 (8) (2004) 1615.
[25] W. Vichit-Vadakan, G.W. Scherer, Measuring permeability and stress relaxation of young cement paste by beam-bending, Cem. Concr. Res. 33 (2003) 1925–1932.
[26] J.J. Valenza II, G.W. Scherer, Measuring permeability of rigid materials by a beam-bending method: V. Isotropic rectangular plates of cement paste, J. Am. Ceram. Soc. 87 (10) (2004) 1927–1931.
[27] G.C. Simmons, "Thermopermeametry of Sand Mortars", Senior thesis, Dept. Civil & Env. Eng., Princeton University, (2005).
[28] P. Debye, R.L. Cleland, Flow of liquid hydrocarbons in porous Vycor, J. Appl. Phys. 30 (6) (1959) 843–849.
[29] M.Y. Lin, B. Abeles, J.S. Huang, H.E. Stasiewski, Q. Zhang, Viscous flow and diffusion of liquids in microporous glasses, Phys. Rev., B 46 (1) (1992) 10701–10705.
[30] P. Levitz, Statistical modeling of pore network, in: K. Sing (Ed.), Handbook of Porous Media, vol. 1, Wiley–VCH, 2002, pp. 37–80.
[31] M.E. Nordberg, Properties of some Vycor-brand glasses, J. Am. Ceram. Soc. 27 (10) (1944) 299–305.
[32] E.J. Sellevold, C.W. Richards, Short-time creep transition for hardened cement paste, J. Am. Ceram. Soc. 55 (6) (1972) 284–289.
[33] G.W. Scherer, H. Hdach, J. Phalippou, Thermal expansion of gels: a novel method for measuring permeability, J. Non-Cryst. Solids 130 (1991) 157–170; Errata, J. Non-Cryst. Solids 194 (1996) 326.
[34] G.W. Scherer, Measuring permeability by the thermal expansion method for rigid or highly permeable gels, J. Sol-Gel Sci. Technol. 3 (1994) 31–40.

[35] G.W. Scherer, Thermal expansion kinetics: method to measure permeability of cementitious materials: I, Theory, J. Am. Ceram. Soc. 83 (11) (2000) 2753–2761;
Erratum, J. Am. Ceram. Soc. 87 (8) (2004) 1609–1610.
[36] H. Ai, J.F. Young, G.W. Scherer, Thermal expansion kinetics: method to measure permeability of cementitious materials: II, application to hardened cement paste, J. Am. Ceram. Soc. 84 (2) (2001) 385–391;
Erratum, J. Am. Ceram. Soc. 87 (8) (2004) 1611.
[37] G.W. Scherer, Thermal expansion kinetics: method to measure permeability of cementitious materials: III, Effect of viscoelasticity, J. Am. Ceram. Soc. 87 (8) (2004) 1509–1516.
[38] J.P. Ciardullo, D.J. Sweeney, G.W. Scherer, Thermal expansion kinetics: method to measure permeability of cementitious materials: IV, effect of thermal gradients, J. Am. Ceram. Soc. 88 (5) (2005) 1213–1221.
[39] J.J. Valenza, G.W. Scherer, Evidence of anomalous thermal expansion of water in cement paste, Cem. Concr. Res. 35 (2005) 57–66.
[40] R.A. Helmuth, Dimensional changes of hardened Portland cement pastes caused by temperature changes, Proc. Highway Res. Board 40 (1961) 315–335.
[41] F. Wittmann, J. Lukas, "Experimental study of thermal expansion of hardened cement paste", Matér. Constr. 7 (4) (1974) 247–252.
[42] H. Ai, J.F. Young, Volume stability of densified cement pastes, in: M. Cohen, S. Mindess, J. Skalny (Eds.), Materials Science of Concrete–Sidney Diamond Symposium, Am. Ceram. Soc., Westerville, OH, 1998, pp. 493–507.
[43] Z.P. Bazant, Delayed thermal dilatations of cement paste and concrete due to mass transport, Nucl. Eng. Des. 14 (1970) 308–318.
[44] J. Gross, G.W. Scherer, Dynamic pressurization: novel method for measuring fluid permeability, J. Non-Cryst. Solids 325 (2003) 34–47.
[45] G.W., Scherer,, "Dynamic Pressurization Method for Measuring Permeability and Modulus: I. Theory", Materials and Structures, doi:10.1617/s11527-006-9124-x (available online).
[46] Z.C. Grasley, G.W. Scherer, D.A. Lange, and J.J. Valenza II, "Dynamic Pressurization Method for Measuring Permeability and Modulus: II. Cementitious materials", Materials and Structures, in press.
[47] Z.C. Grasley, J.J. Valenza II, G.W. Scherer, D.A. Lange, Measuring permeability and bulk modulus of cementitious materials, in: G. Pijaudier-Cabot, B. Gérard, P. Acker (Eds.), Creep, Shrinkage and Durability of Concrete and Concrete Structures, Hermes, London, 2005, pp. 213–218.
[48] F. Skoczylas, O. Coussy, Z. Lafhaj, Sur la fiabilité des mesures des perméabilités hétérogènes par injection de gaz (On the reliability of measurements of heterogeneous permeability by injection of gas), Rev. Fr. Génie Civ. 7 (2003) 4.
[49] G.W. Scherer, Hydraulic radius and mesh size of gels, J. Sol-Gel Sci. Technol. 1 (1994) 285–291.
[50] P.M. Adler, Hydrodynamic transport in and around fractal porous media, Characterization of Porous Solids, Elsevier, Amsterdam, 1988, pp. 433–439.
[51] G.W. Scherer, C. Alviso, R. Pekala, J. Gross, Permeability and structure of re-sorcinol-formaldehyde gels, in: R.F. Lobo, J.S. Beck, S.L. Suib, D.R. Corbin, M.E. Davis, L.E. Iton, S.I. Zones (Eds.), Microporous and Macroporous Materials, MRS Symp. Proc., vol. 431, Mater. Res. Soc., Pittsburgh, PA, 1996, pp. 497–503.
[52] G.W. Scherer, Effect of drying on properties of silica gel, J. Non-Cryst. Solids 215 (2,3) (1997) 155–168.
[53] K.J. Packer, The dynamics of water in heterogeneous systems, Philos. Trans. R. Soc. Lond., B 278 (1977) 59–87.
[54] R. Bruni, M.A. Ricci, A.K. Soper, Water confined in Vycor glass. I. A neutron diffraction study, J. Chem. Phys. 109 (4) (1998) 1478–1485.
[55] P. Gallo, M.A. Ricci, M. Rovere, Layer analysis of the structure of water confined in Vycor glass, J. Chem. Phys. 116 (1) (2002) 342–346.
[56] S.-B. Zhu, G.W. Robinson, Structure and dynamics of liquid water between plates, J. Chem. Phys. 94 (2) (1991) 1403–1410.
[57] A.J. Katz, A.H. Thompson, Quantitative prediction of permeability in porous rock, Phys. Rev., B 34 (11) (1986) 8179–8181.
[58] A.J. Katz, A.H. Thompson, Prediction of rock electrical conductivity from mercury injection measurements, J. Geophys. Res. 92 (B1) (1987) 599–607.
[59] D.L. Johnson, J. Koplik, L.M. Schwartz, New pore-size parameter characterizing transport in porous media, Phys. Rev. Lett. 57 (20) (1986) 2564–2567.
[60] P.N. Sen, Time-dependent diffusion coefficient as a probe of geometry, Concepts Magn. Reson. 23A (1) (2004) 1–21.
[61] C. Pacheco and Sonya Xu, Princeton University, unpublished results.
[62] B.V. Derjaguin, V.V. Karasev, E.N. Khromova, Thermal expansion of water in fine pores, J. Colloid Interface Sci. 109 (2) (1986) 586–587.
[63] S. Xu, G.C. Simmons, G.W. Scherer, Thermal expansion and viscosity of confined liquids, in: J.T. Fourkas, P. Levitz, M. Urbakh, K.J. Wahl (Eds.), Dynamics of Small Confining Systems, Mat. Res. Soc. Symp. Proc., vol. 790, Materials Res. Soc., Warrendale, 2004, pp. 85–91, P.6.8.1–7.
[64] T.S. Mahadavan and S.H. Garofalini, "Molecular dynamics simulations of confined water in silica", J. Phys. Chemistry (in press).
[65] S. Xu, T.S. Mahadavan, S.H. Garofalini, and G.W. Scherer, "Thermal expansion of water in porous glasses", Langmuir (submitted for publication).
[66] P.K. Mehta, D. Manmohan, Pore size distribution and permeability of hardened cement pastes, Proc. 7th Int. Cong. Cement Chem., vol. III, Editions Septima, Paris, 1988, pp. VII-1–VII-5.
[67] B.K. Nyame, J.M. Illston, Capillary pore structure and permeability of hardened cement paste, Proc. 7th Int. Cong. Cement Chem., vol. III, Editions Septima, Paris, 1988, pp. VII-181–VII-185.
[68] A.S. El-Dieb, R.D. Hooton, Evaluation of the Katz–Thosmpson model for estimating the water permeability of cement-based materials from mercury intrusion porosimetry data, Cem. Concr. Res. 24 (3) (1994) 443–455.
[69] E.J. Garboczi, Permeability, diffusivity, and microstructural parameters: a critical review, Cem. Concr. Res. 20 (1990) 591–601.
[70] B.J. Christensen, T.O. Mason, H.M. Jennings, Comparison of measured and calculated permeabilites for hardened cement pastes, Cem. Concr. Res. 26 (9) (1996) 1325–1334.
[71] V. Baroghel-Bouny, M. Mainguy, O. Coussy, Isothermal drying process in weakly permeable cementitious materials — assessment of water permeability, in: R.D. Hooton, M.D.A. Thomas, J. Marchand, J.J. Beaudoin (Eds.), Materials Science of Concrete Special Volume: Ion and Mass Transport in Cement-Based Materials, Am. Ceram. Soc., Westerville, OH, 2001, pp. 59–80.
[72] V. Baroghel-Bouny, private communication.
[73] A.S. El-Dieb, R.D. Hooton, Evaluation of the Katz–Thompson model for estimating the water permeability of cement-based materials from mercury intrusion porosimetry data, Cem. Concr. Res. 24 (3) (1994) 443–455.
[74] P.J. Tumidajski, B. Lin, On the validity of the Katz–Thompson equation for permeabilities in concrete, Cem. Concr. Res. 28 (5) (1998) 643–647.
[75] J.J. Thomas, H.M. Jennings, A.J. Allen, The surface area of hardened cement paste as measured by various techniques, Concr. Sci. Eng. 1 (1999) 45–64.
[76] R.A. Olson, C.M. Neubauer, H.M. Jennings, Damage to the pore structure of hardened Portland cement paste by mercury intrusion, J. Am. Ceram. Soc. 80 (9) (1997) 2454–2458.
[77] W.P. Halperin, J.-Y. Jehng, Y.-Q. Song, Application of spin–spin relaxation to measurement of surface area and pore size distributions in a hydrating cement paste, Magn. Res. Imaging 12 (1994) 169–173.
[78] P.J. Prado, B.J. Balcom, S.D. Beyea, T.W. Bremner, R.L. Armstrong, P.E. Grattan-Bellew, Concrete freeze/thaw as studied by magnetic resonance imaging, Cem. Concr. Res. 28 (2) (1998) 261–270.
[79] S.D. Beyea, B.J. Balcom, T.W. Bremner, R.L. Armstrong, P.E. Grattan-Bellew, Detection of drying-induced microcracking in cementitious materials with space-resolved 1H nuclear magnetic resonance relaxometry, J. Am. Ceram. Soc. 86 (5) (2003) 800–805.
[80] J.P. Korb, D. Petit, S. Philippot, H. Zanni, V. Maret, M. Cheyrezy, Nuclear relaxation of water confined in reactive powder concrete, in: P. Colomber, A.R. Grimmer, H. Zanni, P. Sozzani (Eds.), Nuclear Magnetic Resonance Spectroscopy of Cement-based Materials, 1998, pp. 333–343.
[81] G. Fagerlund, Determination of pore-size distribution from freezing-point depression, Matér. Constr. 6 (33) (1973) 215–225.
[82] M. Brun, A. Lallemand, J.F. Quinson, C. Eyraud, A new method for the simultaneous determination of the size and the shape of pores: the thermoporometry, Thermochim. Acta 21 (1977) 59–88.

[83] J. Villadsen, Pore structure in cement based materials, Tech. Rep., 0908-3871vol. 277, Building Materials Lab., Technical Univ., Denmark, 1992.
[84] P. Colombet, A.-R. Grimmer, H. Zanni, P. Sozzani (Eds.), Nuclear Magnetic Resonance Spectroscopy of Cement-Based Materials, Springer, Berlin, 1998.
[85] E. Derouane, Étude par résonance magnétique nucléaire de haute résolution du pseudo-liquid dans les systèmes adsorbés, Acad. R. Belge., Bull. Ch. Sci. 54 (10) (1968) 1341–1351.
[86] J.-Y. Jehng, D.T. Sprague, W.P. Halperin, Pore structure of hydrating cement paste by magnetic resonance relaxation analysis and freezing, Magn. Res. Imaging 14 (7/8) (1996) 785–791.
[87] G.W. Scherer, D.M. Smith, D. Stein, Deformation of aerogels during characterization, J. Non-Cryst. Solids 186 (1995) 309–315.